Photoinitiating Free-Radical Polymerization Electron-Transfer Pairs Applying Amino Acids and Sulfur-Containing Amino Acids as Electron Donors

Franciszek Ścigalski, Jerzy Pączkowski

Faculty of Chemical Technology and Engineering, University of Technology and Agriculture, Seminaryjna 3, 85-326 Bydgoszcz, Poland

Received 24 February 2003; accepted 9 December 2004
DOI 10.1002/app.21757
Published online in Wiley InterScience (www.interscience.wiley.com).

ABSTRACT: A series of free-radical polymerization initiation systems, based on xanthene dyes as the absorbing chromophores [Rose bengal derivative, 3-(3-methylbutoxy)-5,7-diiodo-6-fluorone and 3-acetoxy-2,4,5,7-tetraiodo-6-fluorone] and sulfur-containing amino acids as the electron donors, were investigated. The photoredox pair xanthene dye/sulfur-containing amino acid was effectively used for photoinitiation of free-radical polymerization of the mixture composed of poly(ethylene glycol)diacrylate–1% NH_4OH (3 : 1). The highest initiating efficiencies were observed for the system composed of methionine derivatives as the electron donor. The mechanism of photoinduced electron transfer between sulfur-containing amino acids and triplet state of xanthene dye was investigated using laser-flash and steady-state photolysis techniques. Based on photochemistry of xanthene dyes, photochemistry of sulfur-containing amino acids, and obtained results, the mechanism describing the major processes occurring during the photoinitiated polymerization by a photoinduced intermolecular electron-transfer process was postulated. © 2005 Wiley Periodicals, Inc. J Appl Polym Sci 97: 358–365, 2005

Key words: photochemistry; photopolymerization; free-radical polymerization; kinetics (polym.); photoinduced intermolecular electron transfer (PET)

INTRODUCTION

Various research groups have studied the photopolymerization of vinyl monomers using as photoinitiators the dyes that absorb in the visible region of the spectrum.[1–4] The photoreduction of xanthene dyes in the presence of electron donors undergoes a photoinduced intermolecular electron transfer (PET) reaction, which is followed by transformations that yield free radicals able to initiate polymerization of vinyl monomers.[2,5]

Free radicals may be produced by the direct photolysis of the photoinitiators. However, this process requires light with a wavelength that is localized in the ultraviolet part of the spectra. Therefore, the panchromatic sensitization of vinyl polymerization requires the presence of a suitable dye as a light absorber. This can either transfer energy or undergo an electron-transfer process, which is possible because its electronically excited state is easier to reduce. On the other hand, a photoredox process requires a proper electron donor. The compounds commonly applied as electron donors are amines.[5–9] For this group of compounds the photoinduced electron-transfer process involves many steps, including an electron transfer between an excited acceptor (A) and an electron donor (HD) followed by a proton transfer from the electron-donor radical cation to the dye radical anion,[5,10] or by other specific secondary reactions, yielding free radicals that are able to start the initiating process. For amino acids the process is more complex and the reactions that follow electron transfer besides proton transfer may involve decarboxylation, which yields different types of free radicals.

Scheme 1 summarizes the possible processes that may occur during the free-radical photoinitiated polymerization by the photoinduced intermolecular electron transfer (PET) process in the presence of the most commonly used electron donors. In Scheme 1, k_{dif} is the rate constant representing the rate of diffusive encounters between reactants, which can dissociate with rate constant k_{-dif}; k_{el} is the first-order rate constant of electron transfer with the reverse step denoted by the rate constant k_{-el}; k_H is the rate constant of proton transfer between ion radicals; the cross-coupling step is designated by the rate constant k_{bl}; the polymerization step is denoted by k_p; and k_{ret} denotes the rate constants for the process of electron return.

In this article, a series of free-radical polymerization initiation systems, based on photoreducible dyes (xan-

Correspondence to: F. Ścigalski (scigal@atr.bydgoszcz.pl).
Contract grant sponsor: State Committee for Scientific Research (KBN); contract grant number: 4-T09A-167 27.

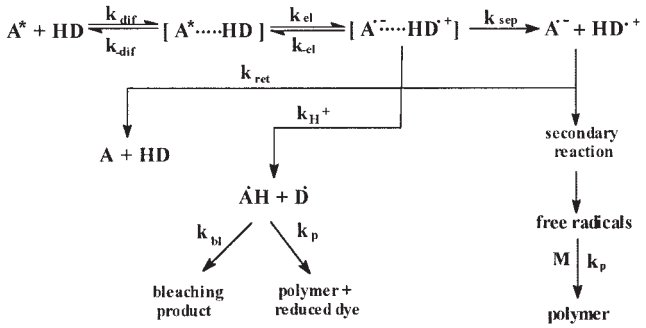

Scheme 1

thene dyes) as the absorbing chromophore and amino acids or sulfur-containing amino acids as the electron donors, are described. A motivation for this work was the desire to study new photoinitiating systems based on xanthene dyes and amino acids or sulfur-containing amino acids, the nonallergy and biologically nontoxic compounds, which can replace harmful compounds as electron donors in many applications, especially the electron donors in dental restorative materials.

EXPERIMENTAL

Monomer, poly(ethylene glycol)diacrylate (PEGDA), and substrates for dye synthesis were purchased from Aldrich (Milwaukee, WI). The amino acids (AAc) and sulfur-containing amino acids (SAAc) were from Aldrich as the best available purity grades and were used without further purification. The light-absorbing chromophores, 3-(3-methylbutoxy)-5,7-diiodo-6-fluorone (DIPF) and 3-acetoxy-2,4,5,7-tetraiodo-6-fluorone (AcTIHF), were synthesized using the methodology given by Tanabe et al.[11] Rose bengal derivative (RBAX) was synthesized according to the method described by Valdes-Aquilera et al.[12]

The oxidation potentials of amino acids and reduction potentials of the dyes were measured using cyclic voltammetry. An electroanalytical MTM System model EA9C-4z (Kraków, Poland) was used for the measurements. A platinum (1-mm) disk electrode was used as the working electrode, a Pt wire constituted the counter electrode, and an Ag–AgCl electrode served as a reference electrode. The measurements were carried out under argon in a 0.1*M* solution of tetrabutylammonium perchlorate in dry acetonitrile.

The kinetics of free-radical polymerization was determined based on a measurement of the rate of heat evolution during polymerization. A semiconducting diode, immersed in a 2-mm-thick layer of a cured sample, was used as a temperature sensor. The temperature signal was transformed with an analog–digital data-acquisition board to a computer.

TABLE I
Structures, Reduction Potentials (E_{red}), and 0-0 Triplet Excited State Transition Energy (E_{00}) of Xanthene Dyes Used as Light-Absorbing Chromophore

Acceptor	Structure	E_{red} (eV)	E_{00} (eV)
3-(3-Methylbutoxy)-5,7-diiodo-6-fluorone (DIPF)	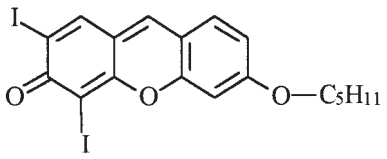	−0.96	2.25
3-Acetoxy-2,4,5,7-tetraiodo-6-fluorone (AcTIHF)	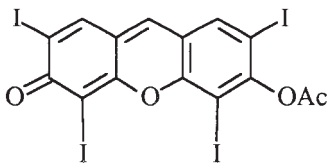	−0.99	2.1
Derivative of Rose bengal (RBAX)	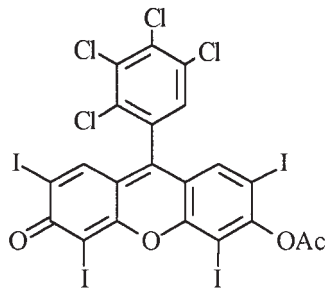	−0.8	2.1

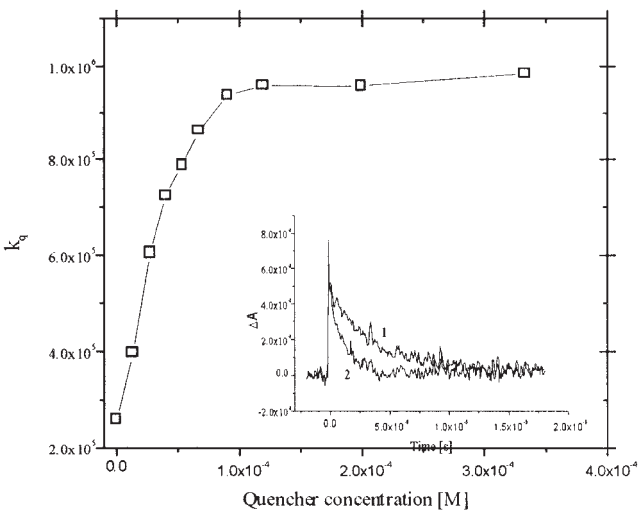

Figure 1 Plots according to eq. (1) for DIPF triplet quenching by thiaproline in MeCN/H_2O solution (3 : 1 v/v). Inset: experimental trace for DIPF triplet decay at 540 nm (curve 1) and DIPF in the presence of thiaproline $3.0 \times 10^{-4}M$ (curve 2).

Photopolymerization was initiated using a model 543-500 MA argon ion laser (two lines of equal intensity at 488 and 514 nm; Omnichrome, Chino, CA). The average power of irradiation was 30 mW/0.785 cm^2. All polymerization procedures were made on one type of formulation, consisting of a mixture of PEGDA–1% NH_4OH in water (7 : 3), a dye (concentration $5 \times 10^{-3}M$), and an electron donor (concentration $0.02M$); pH of the polymerization mixture was 11.8. As a reference sample, a polymerizing formulation without coinitiator was used.

Nanosecond laser-flash photolysis experiments were performed using an LKS.60 laser-flash photolysis apparatus (Applied Photophysics, Ltd., Surrey, UK). Laser irradiation at 355 nm from the third harmonic of the Q-switched Nd : YAG model LPY 150 laser (Lambda Physik AG, Göttingen, Germany), operating at 65 mJ/pulse (pulse width ~ 4–5 ns), was used for the excitation. Transient absorbances at preselected wavelengths were monitored by a detection system consisting of a monochromator, a photomultiplier tube (R955; Hamamatsu Photonics, Hamamatsu City, Japan), and a pulsed xenon lamp (150 W) as a monitoring source. The signal from the photomultiplier was processed by an Agilent Infiniium 54810A digital storage oscilloscope (Hewlett–Packard/Agilent; Palo Alto, CA) and an Acorn-compatible computer.

Concentrations of amino acids and sulfur-containing amino acids in the quenching experiments ranged from 3×10^{-5} to $8 \times 10^{-4}M$. In all experiments, the concentration of xanthene dyes was about $2 \times 10^{-5}M$. Deoxygenation was achieved by bubbling high-purity argon through the solutions.

Decarboxylation of amino acids was controlled with a solution of the xanthene dye ($2.0 \times 10^{-4}M$) and an appropriate amino acid ($5.0 \times 10^{-3}M$) in a 1-cm-diameter tube, which was flushed during irradiation with a stream of carbon dioxide–free argon. The exit gases were passed through three wash bottles in series containing saturated aqueous barium hydroxide. The formation of carbon dioxide was manifested by the formation of barium carbonate precipitate.

RESULTS AND DISCUSSION

The structure, reduction potentials (E_{red}), and triplet excited state–transition energies of studied dyes are compiled in Table I.

Triplet-state quenching of xanthene dyes in the presence of amino acids undergoes a photoinduced intermolecular electron transfer mechanism (PET), which is followed by the transformations that yield the free radicals that, in turn, are able to initiate polymerization.

TABLE II
Quenching Rate Constants of Xanthene Dyes Triplets by Amino Acids and Sulfur-containing Amino Acids (k_q)

			$k_q \times 10^{-9}$ (M^{-1} s^{-1})		
No.	Amino acid	E_{ox} (V)	DIPF (E_{red} = −0.96 V)	AcTIHF (E_{red} = −0.8 V)	RBAX (E_{red} = −0.99 V)
1	DL-Cysteine	0.912	2.89	2.03	3.76
2	DL-Homocysteine	1.140	1.88	0.980	4.15
3	*S*-Methyl-L-cysteine	1.100	3.08	1.69	5.00
4	*S*-Ethyl-L-cysteine	1.164	3.49	2.81	3.07
5	*S*-Carboxymethyl-L-cysteine	0.966	3.15	1.47	3.22
6	*S*-Carboxyethyl-L-cysteine	0.970	3.77	2.01	3.22
7	L-Methionine	1.340	3.56	3.71	6.13
8	Ethionine	1.244	2.54	3.49	4.86
9	*N*-Acetyl-D-methionine	1.016	2.23	2.41	4.80
10	Thiaproline	1.178	9.07	8.76	13.41
11	Glicyne	—	2.43	1.49	5.64
12	Alanine	0.740	2.47	2.65	5.85

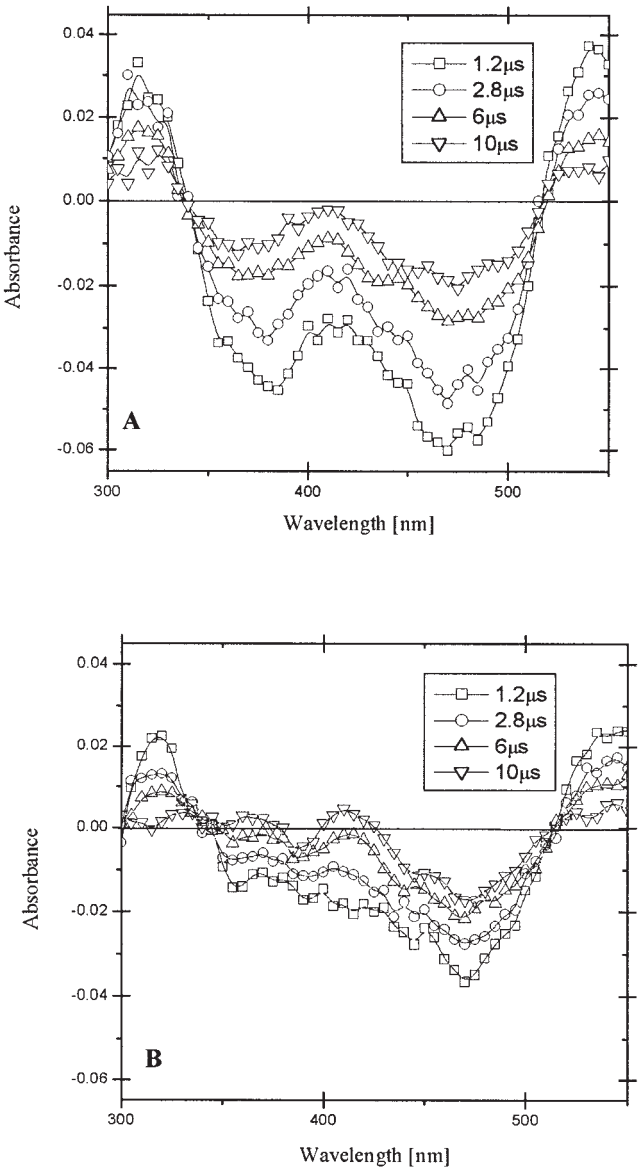

Figure 2 Transient absorption spectra recorded at different delay times: (a) obtained from DIPF ($2 \times 10^{-5}M$) in MeCN + H_2O (3 : 1), and (b) from DIPF ($2 \times 10^{-5}M$) in MeCN + H_2O (3 : 1) in the presence of methionine ($2 \times 10^{-3}M$).

Triplet live-times and quenching rate constants of xanthene dyes by amino acids and sulfur-containing amino acids were studied by means of nanosecond laser-flash photolysis in MeCN or MeCN–water solutions. The quenching rate constants k_{obs} were obtained by monitoring the triplet decays at the maxima of the triplet–triplet absorption spectra of dyes for various quencher concentrations. The resulting pseudo-first-order rate constants k_{obs} were linear at low concentrations of donor and the primary reaction rate constant k_q was obtained from the slope of the following equation:

$$k_{obs} = k^0 + k_q[Q] \quad (1)$$

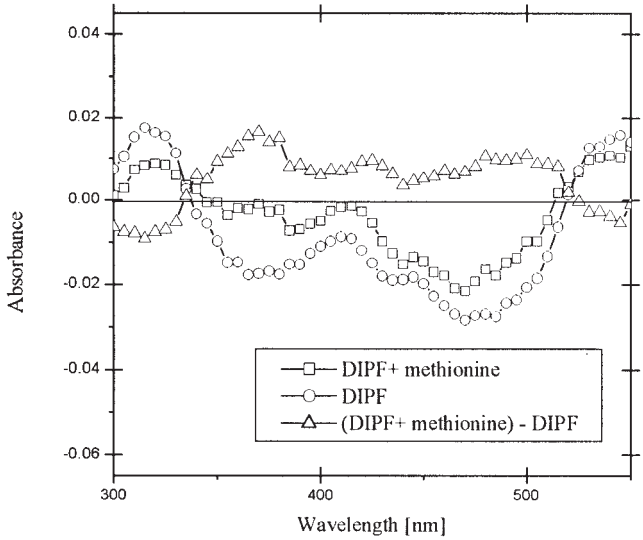

Figure 3 Difference spectrum (6 μs after a laser flash) obtained by subtracting the spectrum of DIPF from the spectrum recorded for DIPF–methionine mixture.

where k^0 is the triplet-state decay rate constant in the absence of an electron donor.

Figure 1 shows results of the quenching experiment along with typical experimental traces, observed for the triplet decay in the presence of a sample amino acid. The quenching rate constants, obtained for all the tested compositions, are listed in Table II.

The laser-flash photolysis spectrum for DIPF (similar to that of AcTIHF and RBAX) is shown in Figure 2(a). The transient absorption spectra of DIPF reveals a typical absorption curve, described earlier by Neckers.[5] The consumption of DIPF is evident in the spectrum from the bleaching of its ground-state absorption band. The spectrum shows a broad absorption band

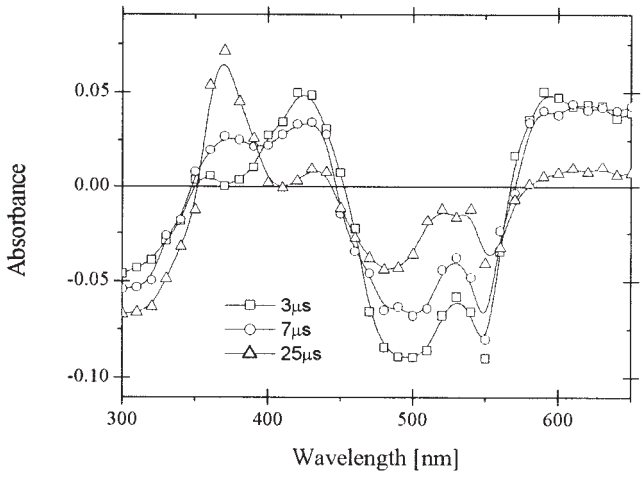

Figure 4 Transients absorption spectra recorded at different delay times for RBAX in the presence of DMABN ($3.2 \times 10^{-3}M$).

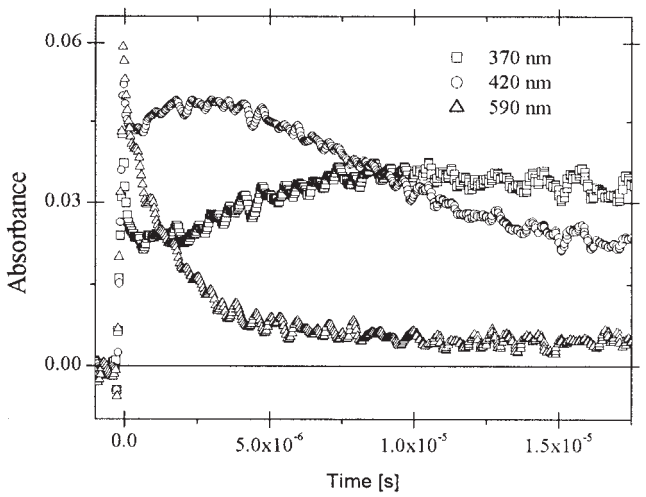

Figure 5 Kinetic traces recorded for intermediates observed in the transient absorption spectra after irradiation of RBAX in the presence of DMABN.

above 500 nm, with the peak at 540 nm for DIPF (580 nm for AcTIHF). This band can be attributed to the triplet–triplet absorption of the xanthene dyes.[5,13,14]

The triplet state of dye in the MeCN solution is the only product, which is indicated by the presence of two isosbestic points at 340 and 510 nm [Fig. 2(a)]. The transient absorption spectra of the DIPF, in the presence of coinitiator (methionine) recorded at different delay times after the flash, are shown in Figure 2(b).

There are no significant changes in the absorption spectra of these transients, with the exception of a slight decrease of the bleaching of the ground-state absorption. However, when compared under identical experimental conditions (see Fig. 3) it is apparent that the changes in absorption suggest the presence of new transients. The difference spectrum obtained by subtracting the spectrum obtained for DIPF from the spectrum recorded for the DIPF–methionine photoredox pair shows new absorption bands with maxima at 370, 420, and about 500 nm. The nature of these transients is best explained by measuring the RBAX transient absorption spectra in the presence of a tertiary aromatic amine, an efficient electron donor. When 4-(dimethylamino)benzonitrile (DMABN) is the electron donor, two products are formed from the RBAX triplet, as indicated by two transients absorbing at 425 and 370 nm (Fig. 4).

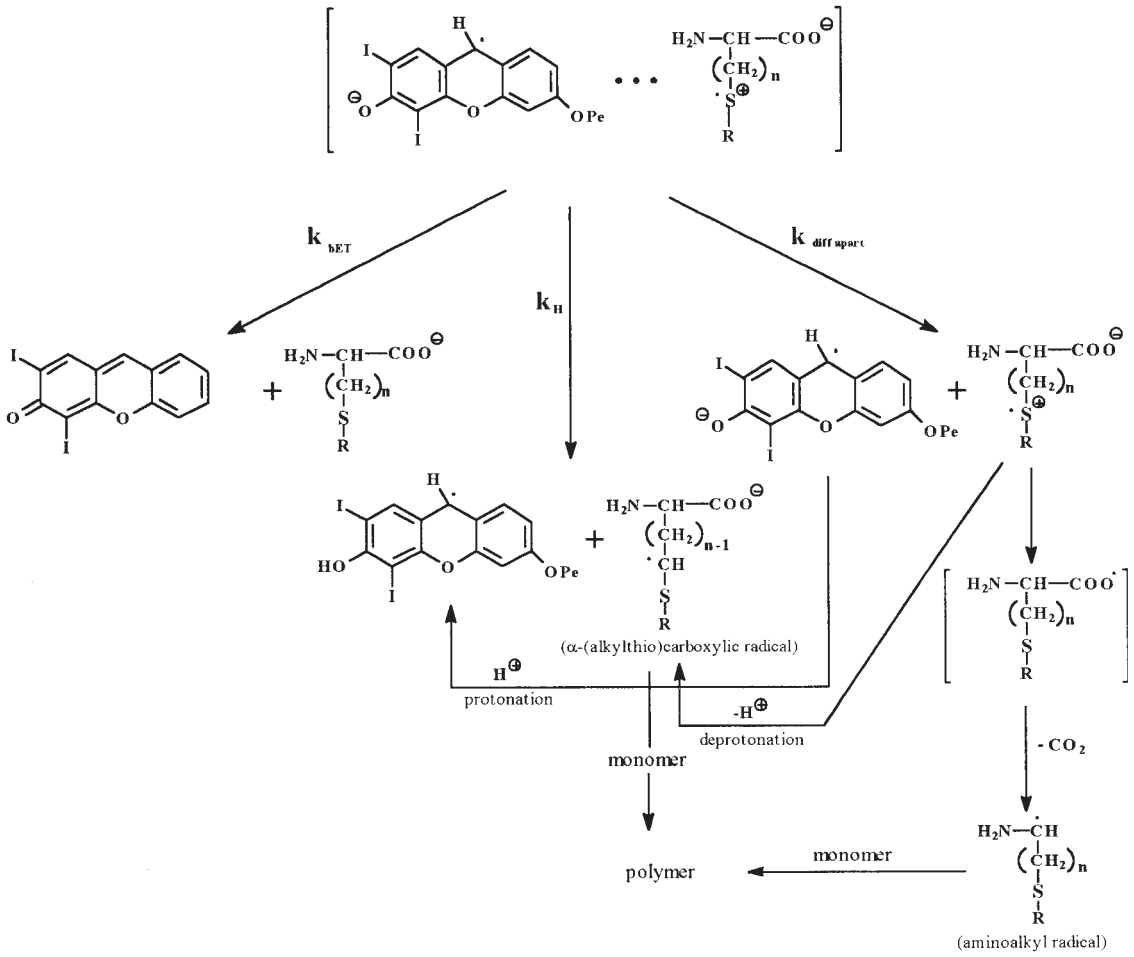

Scheme 2

TABLE III
Presumable Structures of Free Radicals Able to Initiate Free-Radical Polymerization Obtained as a Result of PET Reaction and Relative Rates of PEGDA Polymerization Initiated with Xanthene Dyes–SAAc Composition (pH of polymerizing mixture = 11.8)

No.	Free-radical structures obtained from coinitiator		Rates of polymerization		
			DIPF	AcTIHF	RBAX
1	—	$S—CH_2—\underset{\bullet}{CH}\text{-}COOH$ (NH$_2$)	1.652	0.219	0.049
2	—	$\bullet S—CH_2—CH_2—CH\text{-}COOH$ (NH$_2$)	3.293	0.506	0.064
3	$CH_3—S—CH_2—\underset{\bullet}{CH}$ (NH$_2$)	$CH_3—S—HC(\bullet)—CH—COOH$ (NH$_2$)	3.410	0.554	0.168
4	$CH_3—CH_2—S—CH_2—\underset{\bullet}{CH}$ (NH$_2$)	$CH_3—CH_2—S—CH(\bullet)—CH—COOH$ (NH$_2$)	3.288	0.679	0.161
5	$HOOC—CH_2—CH_2—S—CH_2—\underset{\bullet}{CH}$ (NH$_2$)	$HOOC—CH_2—CH_2—S—CH(\bullet)—CH—COOH$ (NH$_2$)	0.231	0.193	0.027
6	$HOOC—CH_2—CH_2—S—CH_2—\underset{\bullet}{CH}$ (NH$_2$)	$HOOC—CH_2—CH_2—S—CH(\bullet)—CH—COOH$ (NH$_2$)	0.262	0.352	0.029
7	$H_3C—S—CH_2CH_2—\underset{\bullet}{CH}$ (NH$_2$)	$CH_3—S—CHCH_2—\underset{\bullet}{CH}\text{-}COOH$ (NH$_2$)	4.849	0.937	0.235
8	$H_3C—CH_2—S—CH_2—CH_2—\underset{\bullet}{CH}$ (NH$_2$)	$H_3C—CH_2—S—CH(\bullet)—CH_2—CH—COOH$ (NH$_2$)	6.032	0.997	0.483
9	$CH_3—S—CH_2—CH_2—\underset{\bullet}{CH}$ (NH, O C—CH$_3$)	$H_3C—S—\underset{\bullet}{CH}—CH_2—CH\,COOH$ (NH, O C—CH$_3$)	1.516	0.244	—
10	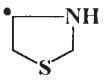	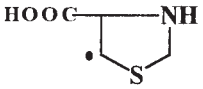	1.338	0.571	0.161
11	$\bullet CH_2—NH_2$	—	4.067	0.937	0.890
12	$H_3C—\underset{\bullet}{CH}—NH_2$	—	1.922	0.185	0.0232

The formation and the decay kinetics of observed intermediates monitored at 370, 420, and 590 nm are shown in Figure 5. From the data in Figure 5 it is clear that the intermediate absorbing at 420 nm increases as the triplet decays (apparent λ_{max} = 590 nm), an observation that suggests that the intermediate absorbing at 420 nm is the primary product of the quenching of RBAX triplet by DMABN. In addition, the formation of the intermediate, monitored at 370 nm, occurs at a rate that is identical (within experimental error) to the rate of decay of the intermediate absorbing at 420 nm. These observations allow us to predict that the final

product of reaction, absorbing at 370 nm, is formed from the intermediate whose peak position is at 420 nm. Additionally, by analyzing the time dependency of the concentration, one can conclude that kinetic traces for all intermediates are characteristic for consecutive elementary reactions, with the triplet state as substrate and the product of reaction absorbing at 370 nm. From the literature it is known that the peak position at 420 nm can be assigned to the RBAX radical ion ($RBAX^{\bullet -}$) and intermediate absorbing at 370 nm to the RBAX neutral radical ($RBAX^{\bullet}$).[5,15–17] Based on the experimental data discussed earlier, one can propose the mechanism that occurs between excited RBAX and DMABN. After initial electron transfer from the amine nitrogen to the dye triplet, the RBAX radical anion ($RBAX^{\bullet -}$) and the amine radical cation pair are obtained. The radical anion promotes proton transfer from the carbon α to the nitrogen of the amino radical cation, yielding the neutral dye radical and the amine neutral radical.

By analogy to the previous discussion with respect to the xanthene dye–methionine photoredox pair (Fig. 3), one can conclude that the transient absorption band at 420 nm can be assigned to the presence of the dye radical anion ($DIPF^{\bullet -}$) and the band at 370 nm to the presence of the dye neutral radical ($DIPF^{\bullet}$). There is one more transient absorption band present in the spectrum shown in Figure 3. This additional absorption band appears at a red region of the transient absorption spectra with the maximum at about 500 nm. According to Hug et al.[18] this transient can be associated with the dimeric cation radical $(S \therefore S)^{+}$ that is formed with a two-center, three-electron bond between the monomeric sulfur radical cation $>S^{\bullet +}$ and the sulfur of unreacted methionine. The presence of absorption bands at 420 and about 500 nm explicitly suggests not only the electron-transfer reaction between xanthene dye and methionine but also that the electron transfer occurs from methionine sulfur to the excited triplet state of xanthene dye.

Based on both the laser-flash photolysis experiments and the results of the supporting steady-state irradiation showing the formation of carbon dioxide, as well as from similar reactions reported for other xanthene dyes and amino acids,[9,16–19] one can conclude that the radicals able to initiate polymerization of monomer result from one-electron photooxidation of a donor (SAAc) according to the sequence of processes summarized in Scheme 2.

After initial electron transfer from sulfur of the sulfur-containing amino acid to the dye triplet, a dye radical anion and a sulfur-centered radical cation pair are obtained. This reaction is followed either by (1) diffusion of the charge-transfer (CT) complex (components of radical ion pair) or by (2) the intramolecular proton transfer within the CT complex, leading to the formation of the α-(alkylthio) carboxylic radical. The first process leads either to the recovery of substrates by back electron-transfer reaction or to the formation of aminoalkyl radical, which arises from the intramolecular electron-transfer reaction from carboxyl group to the sulfur-centered radical cation followed by decarboxylation.

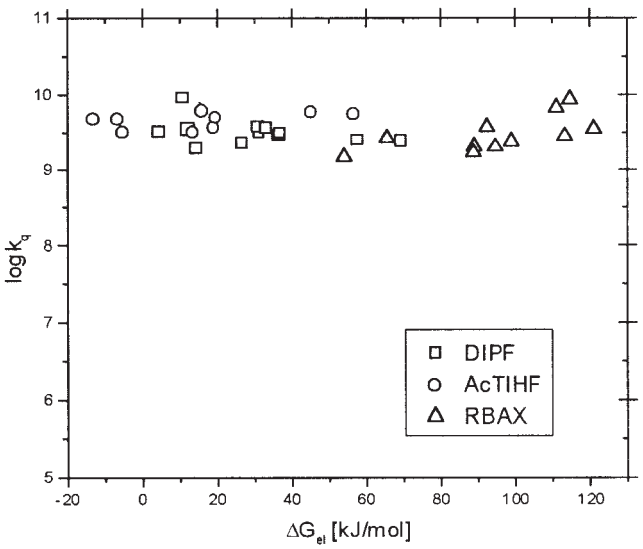

Figure 6 Dependency of the quenching rate constant k_q on ΔG_{el} for quenching of tested xanthene dyes by SAAc.

The structures of free radicals, formed after PET, are possible to predict by analyzing the processes presented in Scheme 2. For the tested sulfur-containing amino acids the presumed structures of free radicals are presented in Table III.

The free energy change ΔG_{el} for the electron-transfer process is calculated by using the Rehm–Weller equation[20,21] as follows:

$$\Delta G_{el} = E_{ox}(D/D^{\bullet +}) - E_{red}(A^{\bullet -}/A) - \frac{\Delta Z e^2}{D r_{1,2}} - E_{00} \quad (2)$$

where $E_{ox}(D/D^{\bullet +})$ is the oxidation potential of the electron donor (SAAc), $E_{red}(A^{\bullet -}/A)$ is the reduction potential of the electron acceptor (dyes), and E_{00} is the triplet excitation energy, which should correlate with the obtained electron transfer rates. The coulombic energy $-(\Delta Z e^2/D r_{1,2})$, considered to be negligible compared to the overall magnitude of ΔG in the present system, is the free energy gained by bringing the radical ions formed to an encounter distance in a solvent with dielectric constant ε.

Data presented in Figure 6 show that, for the photoredox pairs under investigation, the quenching rate constant k_q does not vary when the thermodynamic driving force $(-\Delta G_{el})$ for electron transfer increases, which suggests that the electron-transfer process is controlled by diffusion. Thus, the variation of photoinitiation ability of free-radical polymerization for var-

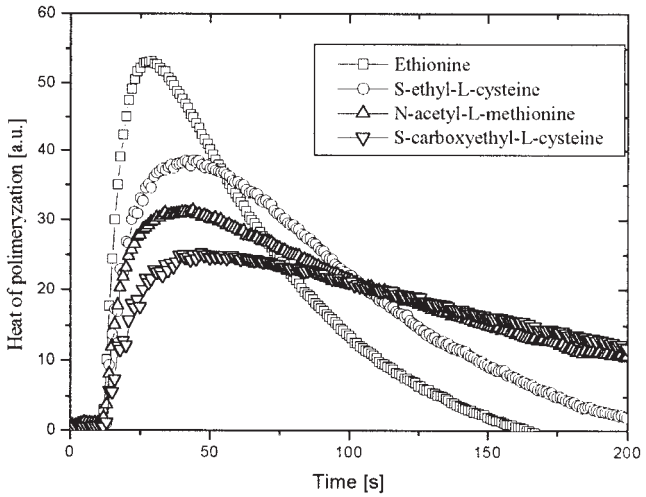

Figure 7 Kinetic curves recorded during photoinitiated polymerization of PEGDA with DIPF as the initiating dye and selected amino acids used as electron donors.

ious photoredox pairs, if observed, will derive from the different reactivities of obtained free radicals.

CONCLUSIONS

Photoinitiated polymerization experiments were carried out to compare the relationship between the photoredox pair structure and the efficiency of photopolymerization. Figure 7 shows the kinetic curves of photoinitiated polymerization of PEGDA obtained for DIPF as the initiating dye and selected sulfur-containing amino acids. The initial rates of photoinitiated polymerization for tested photoinitiating systems are summarized in Table III.

Inspection of the data listed in Table III indicates that the best relative rate of free-radical polymerization for all tested xanthene dyes is observed for the formulation containing ethionine or methionine as the electron donor. For the polymerization mixture containing cysteine derivatives, or alanine (amino acid without sulfur in the molecule, applied for comparison), the rate of polymerization is low and is even lower for alanine acting as electron donor. Because the rate of electron transfer for the entire series of donor–acceptor pairs is similar, to explain the variation in photoinitiation ability of photoredox pairs, different reactivities of free radicals resulting from the PET reaction can be assumed.

This work was supported by State Committee for Scientific Research (KBN) under Grant 4-T09A-167 27.

References

1. Shi, J.; Zhang, X. P.; Neckers, D. C. J Org Chem 1992, 57, 4418.
2. Polikarpow, A. Y.; Hassoon, S.; Neckers, D. C. Macromolecules 1996, 29, 8274.
3. Neumann, M. G.; Rodriques, M. R. Polymer 1998, 39, 1657.
4. Rodriques, M. R.; Catalina, F.; Neumann, M. G. Photochem Photobiol A: Chem 1999, 124, 29.
5. Hassoon, S.; Neckers, D. C. J Phys Chem 1995, 99, 9416.
6. Inbar, S.; Linschitz, H.; Cohen, S. G. J Am Chem Soc 1980, 102, 1419.
7. Cook, W. D. Polymer 1992, 33, 600.
8. Paczkowski, J.; Pietrzak, M.; Kucybała, Z. Macromolecules 1996, 29, 5057.
9. Kabatc, J.; Kucybała, Z.; Pietrzak, M.; Cigalski, F.; Paczkowski, J. Polymer 1999, 40, 735.
10. Klimczuk, E.; Rodgers, M. A.; Neckers, D. C. J Phys Chem 1992, 96, 9817.
11. Tanabe, T.; Torres-Filho, A.; Neckers, D. C. J Polym Sci Part A: Polym Chem 1995, 33, 1691.
12. Valdes-Aquilera, O.; Pathac, C. P.; Shi, J.; Watson, D.; Neckers, D. C. Macromolecules 1992, 95, 541.
13. Grossweiner, L. I.; Zwicer, E. F. J Chem Phys 1961, 34, 1411.
14. Wintgens, V.; Scaiano, J. C.; Linden, S. M.; Neckers, D. C. J Org Chem 1989, 54, 5242.
15. Kasche, V.; Linqvist, L. J Phys Chem 1967, 68, 817.
16. Kasche, V.; Linqvist, L. J Photochem Photobiol 1967, 4, 923.
17. Klimtchuk, E.; Rodgers, M. A. J.; Neckers, D. C. J Phys Chem 1992, 96, 9817.
18. Hug, G. L.; Bobrowski, K.; Kozubek, H.; Marciniak, B. Photochem Photobiol 1998, 68, 785.
19. Zhang, X. P.; Neckers, D. C. J Org Chem 1993, 58, 2614.
20. Rehm, D.; Weller, A. Ber Bunsen-Ges Phys Chem 1969, 73, 834.
21. Rehm, D.; Weller, A. Isr J Chem 1970, 8, 259.